



Since January 2020 Elsevier has created a COVID-19 resource centre with free information in English and Mandarin on the novel coronavirus COVID-19. The COVID-19 resource centre is hosted on Elsevier Connect, the company's public news and information website.

Elsevier hereby grants permission to make all its COVID-19-related research that is available on the COVID-19 resource centre - including this research content - immediately available in PubMed Central and other publicly funded repositories, such as the WHO COVID database with rights for unrestricted research re-use and analyses in any form or by any means with acknowledgement of the original source. These permissions are granted for free by Elsevier for as long as the COVID-19 resource centre remains active.



Growth restriction of an experimental live attenuated human parainfluenza virus type 2 vaccine in human ciliated airway epithelium in vitro parallels attenuation in African green monkeys

Anne Schaap-Nutt^{a,1}, Margaret A. Scull^{b,c,1}, Alexander C. Schmidt^a,
Brian R. Murphy^a, Raymond J. Pickles^{b,c,*}

^a Laboratory of Infectious Diseases, RNA Viruses Section, National Institute of Allergy and Infectious Diseases, National Institutes of Health, Department of Health and Human Services, Bethesda, MD 20892-2007, USA

^b Cystic Fibrosis/Pulmonary Research and Treatment Center, University of North Carolina at Chapel Hill, Chapel Hill, NC 27599-7248, USA

^c Department of Microbiology and Immunology, University of North Carolina at Chapel Hill, Chapel Hill, NC 27599-7248, USA

ARTICLE INFO

Article history:

Received 3 September 2009
Received in revised form 13 January 2010
Accepted 21 January 2010
Available online 20 February 2010

Keywords:

Human parainfluenza virus
Live attenuated vaccine candidate
Human ciliated airway epithelium

ABSTRACT

Human parainfluenza viruses (HPIVs) are common causes of severe pediatric respiratory viral disease. We characterized wild-type HPIV2 infection in an in vitro model of human airway epithelium (HAE) and found that the virus replicates to high titer, sheds apically, targets ciliated cells, and induces minimal cytopathology. Replication of an experimental, live attenuated HPIV2 vaccine strain, containing both temperature sensitive (*ts*) and non-*ts* attenuating mutations, was restricted >30-fold compared to rHPIV2-WT in HAE at 32 °C and exhibited little productive replication at 37 °C. This restriction paralleled attenuation in the upper and lower respiratory tract of African green monkeys, supporting the HAE model as an appropriate and convenient system for characterizing HPIV2 vaccine candidates.

© 2010 Elsevier Ltd. All rights reserved.

1. Introduction

Human parainfluenza virus type 2 (HPIV2) is an enveloped, single-stranded, non-segmented, negative-sense RNA virus of the *Rubulavirus* genus in the *Paramyxoviridae* family [1]. Similar to respiratory syncytial virus (RSV), influenza virus, HPIV1 and HPIV3, HPIV2 is an important cause of severe lower respiratory tract disease, including croup, bronchiolitis and pneumonia, in children less than 6 years old. HPIVs account for up to 18% of all pediatric hospitalizations for respiratory tract diseases, with HPIV2 alone estimated to be responsible for approximately 3% [2,3]. In addition, HPIV2 causes significant morbidity in infants and children that requires medical attention but not hospitalization [2,4]. Licensed vaccines are currently not available for any HPIV, despite their significant impact on public health.

Our goal is to develop a cDNA derived, live attenuated HPIV2 vaccine that is safe, genetically stable, and protective against lower

respiratory tract disease in young children. The live attenuated vaccine strategy offers several advantages over inactivated or sub-unit formulations, including the ability to elicit broadly protective immune responses consisting of local and serum antibodies as well as CD4+ and CD8+ T cell responses [5]. Furthermore, live attenuated vaccines administered intranasally replicate in the respiratory tract in the presence of maternal antibody, permitting immunization of young infants, and cause an acute, self-limited infection that is readily eliminated from the respiratory tract [5,6]. Finally, intranasal administration of live attenuated virus vaccines induces mucosal antigen-specific immune responses in the upper respiratory tract (URT), which have a major impact on limiting replication of respiratory viruses in the airways [7,8]. Several cDNA derived, intranasally administered live attenuated virus vaccines have been evaluated in clinical trials and were found to be safe and immunogenic, including the licensed influenza virus vaccine (FluMist[®]) and investigational vaccines against HPIV3 (rHPIV3cp45) and RSV (rA2cp248/404/1030ΔSH) [6,9–13].

The development of in vitro and in vivo tests to identify live attenuated respiratory virus vaccine candidates that will exhibit a satisfactory balance between attenuation and immunogenicity in humans is needed. Extensive in vivo studies are often performed during preclinical vaccine development since cell lines generally do not accurately reveal the level of attenuation of viral vaccine candidates for the respiratory tract of humans. Furthermore, the

* Corresponding author at: Cystic Fibrosis/Pulmonary Research and Treatment Center, UNC School of Medicine, 7023 Thurston-Bowles, University of North Carolina at Chapel Hill, Chapel Hill, NC 27599-7248, USA. Tel.: +1 919 966 7044; fax: +1 919 966 5178.

E-mail address: raymond_pickles@med.unc.edu (R.J. Pickles).

¹ These authors contributed equally to this study.

restricted host range of human paramyxoviruses requires the use of non-human primates, a limited and expensive resource, to assess the level of attenuation. Therefore, the availability of an in vitro tissue culture model system that reflects the restriction of replication of attenuated human respiratory viruses in non-human primates and ultimately humans would be desirable for preclinical development of such live attenuated virus vaccines. Using an in vitro system, the level of attenuation of multiple vaccine candidates could be rapidly assessed and suitable vaccine candidates could be selected for further evaluation in non-human primates and in humans.

HPIVs and RSV replicate primarily, if not exclusively, in epithelial cells of the respiratory tract unless the individual is severely immunocompromised [14–17]. In vitro models of human ciliated airway epithelium (HAE) derived from freshly isolated human airway cells and grown at an air–liquid interface have been shown to closely mimic the morphological and physiological characteristics of the human airway epithelium in vivo, including mucociliary transport [18,19]. Furthermore, such HAE models have been used to investigate characteristics of viral infection for a number of respiratory viruses, including human coronaviruses, influenza A viruses, RSV, HPIV1 and HPIV3 [20–25]. Although each of these viruses infects ciliated cells in this model, the consequences of infection vary. For example, infection by influenza A viruses causes extensive early cytopathology in HAE [24,26], whereas RSV, HPIV1 and HPIV3 do not cause overt early cytopathology [20–22]. The ciliated cell tropism of these viruses and the critical role of ciliated cells in innate airway defense suggest a central role for ciliated cells in virus replication and spread with likely adverse consequences for the function of the epithelium of the respiratory tract [20–22].

We propose that HAE culture models may be used to assess restriction of replication in vitro that will parallel restricted replication and attenuation of illness in the human host. We have chosen to test the utility of HAE to estimate the level of attenuation of a live attenuated cDNA derived HPIV2 vaccine candidate designated here as rHPIV2-VAC. This vaccine candidate has been administered to the upper and lower respiratory tract of African green monkeys (AGMs) and is currently in phase 1 clinical trials. rHPIV2-VAC was designed to contain three attenuating elements: a T to C substitution at nucleotide 15 in the 3' genomic promoter (15^{T-C}); a substitution in the viral polymerase (L^{Y948L}); and a deletion in the polymerase ($L^{\text{del}1724}$) [27–29]. The 15^{T-C} mutation was originally identified as a spontaneous mutation following in vitro passage of wild-type (WT) HPIV2 in LLC-MK2 cells. This mutation is non-temperature sensitive (non-*ts*) and efficiently attenuates the virus in both the upper (URT) and lower (LRT) respiratory tract of AGMs as well as in the LRT of hamsters [29]. The L^{Y948L} mutation was originally identified as a *ts* attenuating mutation in the L polymerase of the HPIV3cp45 vaccine candidate [30]. The stability of the mutant HPIV2 L^{Y948L} sequence was enhanced by genetically engineering a codon assignment that would require three nucleotide changes to revert to the original, wild-type tyrosine amino acid assignment [27]. This substitution mutation in HPIV2 resulted in *ts* and *att* phenotypes with restriction of replication observed in the LRT of AGMs and hamsters [27,29]. Lastly, deletion of codons 1724 and 1725 in L of HPIV2 ($L^{\text{del}1724}$) increased the level of temperature sensitivity and attenuation of rHPIV2 bearing the 15^{T-C} and L^{Y948L} mutations and should confer a more stable attenuation phenotype than the point mutation from which it was derived (a L^{S1724I} *att* point mutation in bovine PIV3) [27,30]. The rHPIV2-VAC vaccine candidate virus, containing the above mutations, was found to be *ts* in vitro, with a replication shut-off temperature of 37 °C, and manifested restricted replication in the URT and LRT of AGMs [29]. The mean peak titer of rHPIV2-VAC was reduced 60-fold in the URT and 4000-fold in the LRT of infected AGMs compared to that of rHPIV2-WT [29]. rHPIV2-VAC induced a moderate rise in HPIV2

hemagglutination-inhibiting (HAI) antibodies in AGMs and immunization protected AGMs against wild-type HPIV2 challenge in both the UTR and LRT [29].

In the present study, we utilized HAE cultures to first characterize rHPIV2-WT infection of the human ciliated airway epithelium with respect to level and duration of replication, cell tropism, polarity of infection, cytopathology, and cellular response to infection. Our data demonstrate that HPIV2 infects ciliated cells only, that virus is released from the apical surface only, and that productive replication takes place in the absence of early gross morphological changes to the epithelium. Efficient replication of rHPIV2-WT in HAE allowed us to compare the level of restriction of replication of rHPIV2-VAC in HAE to that previously observed in AGMs. The restriction of replication of rHPIV2-VAC versus rHPIV2-WT in HAE at 32 and 37 °C correlated closely with that seen in the URT and LRT, respectively, of AGMs. Ongoing clinical trials will provide the vaccine virus replication data in seronegative children that is needed to assess the utility of the HAE system in identifying live HPIV2 vaccine viruses that are appropriately attenuated.

2. Materials and methods

2.1. Cells and viruses

Human airway tracheobronchial epithelial cells were isolated from airway specimens of patients without underlying lung disease. Tissues were provided by the National Disease Research Interchange (NDRI, Philadelphia, PA) or by the UNC Cystic Fibrosis Center Tissue Culture Core as excess tissue following lung transplantation according to protocols approved by the Institutional Review Board of the University of North Carolina at Chapel Hill. Primary cells derived from single patient sources were first expanded on plastic and then plated on collagen-coated, permeable Transwell-COL (12-mm diameter) supports at a density of 3×10^5 cells per well. HAE cultures were grown in custom media with provision of an air–liquid interface (ALI) for 4–6 weeks to form differentiated, polarized cultures that resemble in vivo pseudostratified mucociliary epithelium, as previously described [19]. Rhesus monkey LLC-MK2 cells (ATCC CCL 7.1) and human HEp-2 cells (ATCC CCL 23) were maintained in OptiMEM I (Gibco-Invitrogen, Inc., Grand Island, NY) supplemented with 5% FBS and gentamicin sulfate (50 µg/ml).

The HPIV2 recombinants described here are based on the biologically derived HPIV2 strain V9412-6 (V94), which was isolated from a nasal wash specimen from an infected infant and was kindly provided by Dr. Peter Wright of Vanderbilt University. The sequence for the V94 strain was determined previously (Genbank accession #AF533010). The rHPIV2-WT virus was derived from an antigenomic cDNA copy of the HPIV2 V94 genome [4]; the genome of the rHPIV2-VAC vaccine virus is engineered from rHPIV2-WT, as described previously [27–29]. rHPIV2-VAC, which was referred to in our previous publication as rHPIV2-15C/948L/ Δ 1724 [29], contains three attenuating elements: a mutation at nucleotide 15, 15^{T-C} , in the 3' genomic promoter; a substitution in L, L^{Y948L} ; and a six nucleotide deletion in L, $L^{\text{del}1724}$. rHPIV1-WT was derived from HPIV1 strain Washington/20993/1964 [31,32]. Media used for HPIV1 propagation in LLC-MK2 cells contained 1.2% TrypLE Select, a recombinant trypsin-like protease (Gibco-Invitrogen, Inc.), to activate the HPIV1 F protein.

Purified virus stocks were obtained by infecting LLC-MK2 cells and purifying virus in the cell culture supernatant by centrifugation and banding in discontinuous 30/60% (w/v) sucrose gradients in order to minimize contamination by cellular factors. Virus titers were determined by 10-fold serial dilution on LLC-MK2 cells in 96-well plates. After 7 days at 32 °C and 5% CO₂, infection was detected by hemadsorption with guinea pig erythrocytes [28,33].

Viral titers are expressed as 50% tissue culture infectious dose per ml (\log_{10} TCID₅₀/ml).

2.2. Viral inoculation of HAE

The apical surfaces of HAE cultures were washed with phosphate-buffered saline (PBS) to limit the effects of apical secretions on inocula, and fresh media was supplied to the basolateral compartments prior to inoculation. HPIV viruses diluted in culture medium were applied to either the apical or basolateral surface of HAE at a MOI of 5.0TCID₅₀/cell or 1.0TCID₅₀/cell in a 200 μ l inoculum. After incubation for 2 h at either 32 or 37 °C, the inoculum was removed, and cells were washed three times for 5 min each with PBS and then incubated at 32 or 37 °C. Virus released into the apical compartment was harvested by performing apical washes with 425 μ l of media for 30 min at 32 or 37 °C. Basolateral samples were collected directly from the basolateral compartment and the removed volume replaced with fresh media. Samples were collected at 0, 8, 24, 48, 72, 96, and 144 h post-inoculation and stored at –80 °C until analysis.

2.3. Kinetics of rHPIV2 replication in LLC-MK2 cells

Confluent monolayer cultures of LLC-MK2 cells in 6-well plates were infected in triplicate at a MOI of 5.0TCID₅₀/cell. After incubation for 1 h with virus, cultures were washed three times and incubated at 32 or 37 °C, as indicated. Medium from each well was harvested and replaced with fresh medium at 24 h intervals and stored at –80 °C until analysis. Virus present in each sample was quantified by titration on LLC-MK2 cells and detected by hemadsorption.

2.4. En face staining and fluorescence microscopy

HAE were fixed overnight at 4 °C in methanol:acetone (50/50) and then permeabilized with 2.5% Triton X-100. The fixed cells were blocked with 3% bovine serum albumin (BSA) in PBS⁺⁺ (containing 1 mM CaCl₂ and 1 mM MgCl₂) prior to incubating the apical surfaces with antibodies diluted in 1% BSA. HPIV2-positive cells were detected using anti-HPIV2 antibodies obtained from fluid present in subcutaneous chambers of rabbits immunized with purified rHPIV2-WT (1:100 dilution, neutralizing antibody titer of 1:7000), as described previously [34], followed by addition of fluorescein isothiocyanate (FITC)-conjugated goat anti-rabbit IgG (1:500 dilution; Jackson ImmunoResearch Laboratories, Inc., West Grove, PA). HPIV1-positive cells were detected using rabbit anti-HPIV1 antibody, as described previously [20]. Images were acquired using a Leica DMIRD inverted fluorescence microscope equipped with a cooled color charge-coupled device digital camera (MicroPublisher; Q-Imaging, Burnaby, British Columbia, Canada). The percentage of the epithelium positive for viral antigen as an index of percentage of infected cells was quantified over 5 images per culture by black and white pixilation of each image and computer calculation of percent black pixels after inverting the image. This technique determines percentage of black pixels in a defined area and does not account for differences in fluorescent intensity.

2.5. Histology and immunostaining

HAE fixed in methanol:acetone were embedded in paraffin and prepared as 5 μ m histological sections. Sections were stained with hematoxylin and eosin (H&E) or Alcian blue-PAS for analysis by light microscopy or were subjected to standard immunofluorescence protocols. For immunofluorescence, sections were blocked

with 3% BSA in PBS⁺⁺ and then incubated with primary antibodies, rabbit anti-HPIV2 antibodies (1:100) and mouse anti-acetylated alpha tubulin (1:2000; Zymed, San Francisco, CA), diluted in 1% BSA. Primary antibodies were detected with FITC-conjugated goat anti-rabbit IgG and Rhodamine Red-conjugated goat anti-mouse IgG2b (Jackson ImmunoResearch Laboratories, Inc.) diluted 1:500. After washing, cells were overlaid with FluorSave mounting medium (EMD Chemicals, Inc.).

2.6. Type I IFN bioassay

The amount of type I IFN produced in response to viral infection of HAE was determined by a previously described IFN bioassay method [20,35]. Briefly, apical wash samples were pH 2.0-treated to inactivate virus and acid-labile type II IFN, then serially diluted 2-fold on HEp-2 cells alongside a human IFN- β standard (5000 pg/ml; Avonex; Biogen, Inc., Cambridge, MA). After 24 h, cells were infected with recombinant vesicular stomatitis virus (VSV-GFP), obtained from John Hiscott [36]. GFP expression was measured using a Typhoon 8600 scanner (Molecular Dynamics Inc., Sunnyvale, CA). The dilution at which the number of GFP-positive cells approximated 50% of that for untreated wells was considered the end point and compared to the end point of the IFN- β standard to calculate the concentration of type I IFN in each sample.

2.7. Adenylate kinase cytotoxicity assay

Cellular toxicity due to HPIV2 infection was determined by measuring the amount of adenylate kinase (AK) leakage into the apical compartment of HAE. AK is an intracellular enzyme released from cells only when cell membranes are disrupted and has previously been shown to correlate with the proportion of dead or damaged cells after virus infection [37]. To measure cytotoxicity in HPIV2-infected HAE, aliquots of the apical wash samples collected at each time point were centrifuged immediately after collection to eliminate cell debris prior to freezing the sample supernatant. AK concentrations were determined in the apical wash supernatant samples using the ToxiLight BioAssay kit (Lonza Rockland, Inc., Rockland, ME) according to the manufacturer's directions. AK activity upon reaction with the ToxiLight reagent was detected using a luminescence microplate reader and SoftMax Pro software (Molecular Devices, Sunnyvale, CA).

2.8. Replication of rHPIV2 mutants in the respiratory tract of AGMs

Studies in HPIV2 seronegative African green monkeys (AGMs) were previously reported for 11 AGMs infected with rHPIV2-WT and 4 AGMs infected with rHPIV2-VAC [29]. This historical data was combined with data from additional AGM studies to yield larger groups and more accurate comparisons ($n=21$ for rHPIV2-WT, $n=16$ for rHPIV2-VAC). The AGMs were inoculated intranasally and intratracheally with $10^{6.0}$ TCID₅₀ of recombinant HPIV2 at each site and nasopharyngeal swabs and tracheal lavage samples were collected for up to 10 days as described previously [29]. The virus titer in each sample was determined by serial dilution on LLC-MK2 monolayers at 32 °C as described above. The lower limit of detection was 0.5 \log_{10} TCID₅₀/ml.

3. Results

3.1. Characterization of HPIV2 infection in primary cultures of human ciliated airway epithelium

Wild-type HPIV2 (rHPIV2-WT) infection in an in vitro model of the human ciliated airway epithelium (HAE) was first character-

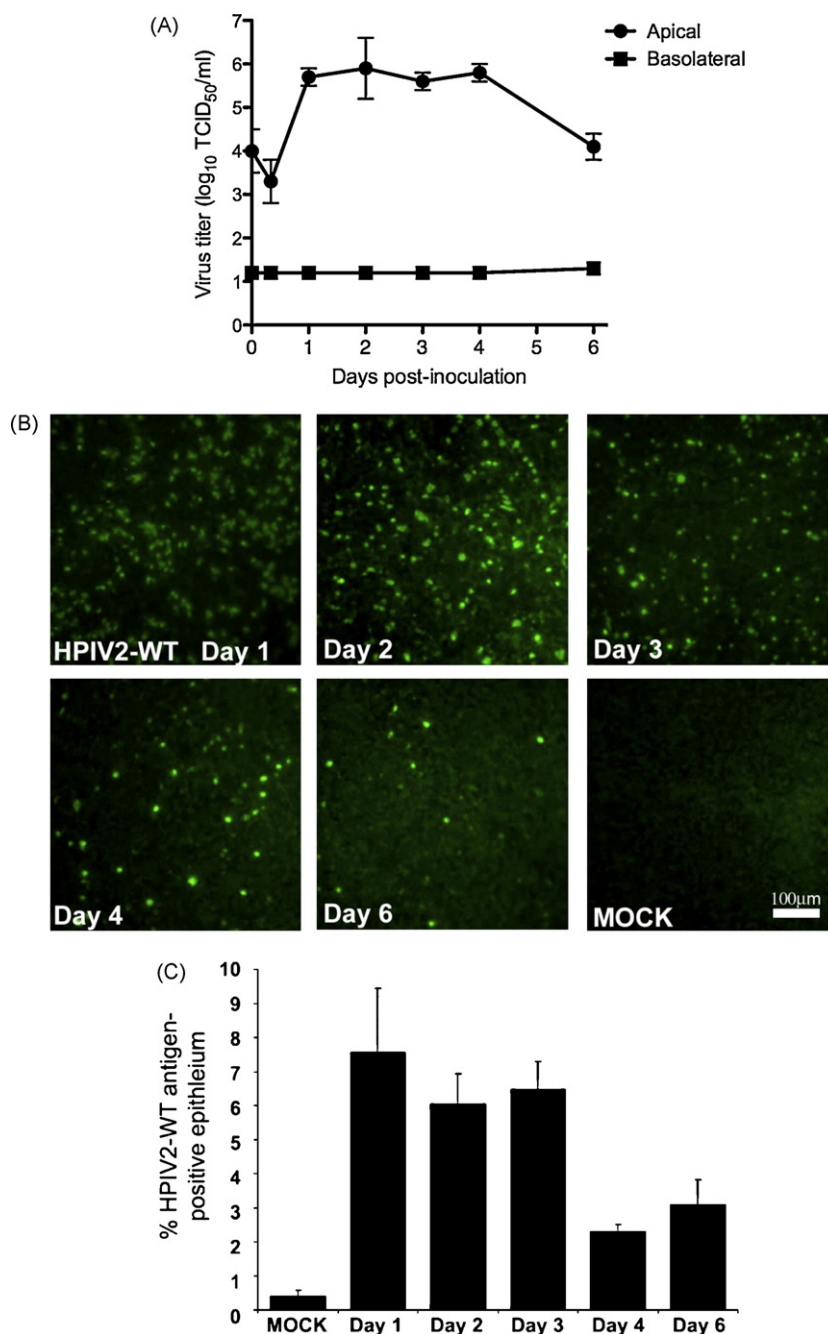
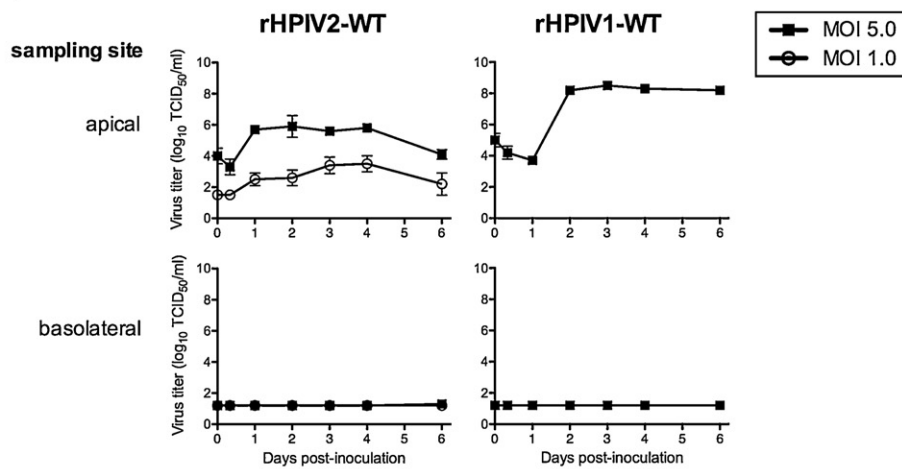
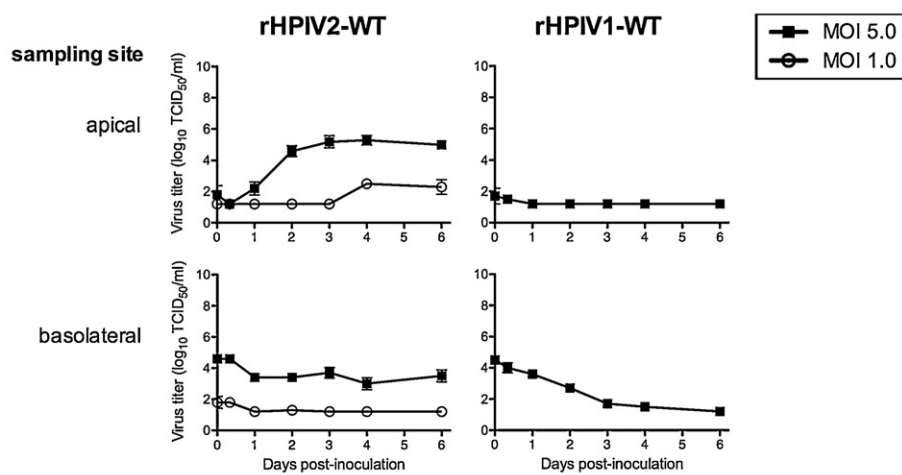


Fig. 1. rHPIV2-WT infects HAE and progeny virus is shed from the apical surface. HAE were inoculated via the apical surface with rHPIV2-WT at high MOI (5.0 TCID₅₀/cell). (A) Titers of virus shed into the apical (circles) and basolateral (squares) compartments were determined at the indicated times. Virus titers shown are the means of 6 cultures from 2 donors (3 cultures per donor) ± S.E. The limit of detection is 1.2 log₁₀ TCID₅₀/ml. (B) Representative photomicrographs of HAE fixed at the indicated times post-inoculation (pi) and immunoprobed *en face* for the presence of HPIV2 antigen (green) after apical inoculation by HPIV2 or vehicle alone (Mock). (C) Quantification of the percentage of HPIV2-positive cells in HAE (FITC-positive surface area) per culture over time after apical inoculation with rHPIV2-WT. Mean across 10 fields ± S.E.

ized. HAE were inoculated at the apical surface with rHPIV2-WT at high MOI (5.0 TCID₅₀/cell), and apical and basolateral compartments were assessed for progeny virus release over time. Quantification of virus in the apical compartment provided evidence of rapid and robust replication and apical shedding of progeny rHPIV2-WT in HAE. Titers of rHPIV2-WT increased 100-fold within the first 24 h following apical inoculation and reached a peak titer of approximately 10⁶ TCID₅₀/ml in the apical wash samples by day 2 post-inoculation (pi) (Fig. 1A), indicating rHPIV2-WT was able to productively infect HAE. In contrast to the high levels of virus detected in the apical wash, little or no virus was measured

above the limit of detection in the basolateral compartment at any time point (Fig. 1A).

The growth kinetics of HPIV2 measured as virus release into the apical compartment correlated well with the number of cells staining positive for viral antigen by *en face* immunostaining for HPIV2 antigen (Fig. 1B and C). By day 1 pi, viral antigen was detected in cells dispersed across the surface of HAE. However, despite high MOI inoculation, on average, only 8–10% of the surface epithelial cells were positive for viral antigen, indicating that only a minority of HAE cells were infected by the initial inoculum. Since rHPIV2-WT appears to infect primarily ciliated cells

(A) **Apical Inoculation****Basolateral Inoculation**

(B)



Fig. 2. rHPIV2-WT, but not rHPIV1-WT, infects HAE via the basolateral surface. (A) HAE was inoculated via the apical surface (top panels) or basolateral surface (bottom panels) with rHPIV2-WT at a MOI of 1.0 or 5.0 TCID₅₀/cell or with rHPIV1-WT at a MOI of 5.0 TCID₅₀/cell. Titers of virus shed into the apical and basolateral compartments were determined at the indicated times pi. The limit of detection is 1.2 log₁₀TCID₅₀/ml. (B) Representative photomicrographs of HAE fixed at day 6 pi and immunoprobed *en face* for the presence of viral antigen (green) after basolateral inoculation with either HPIV2 or HPIV1, or after apical inoculation with HPIV1.

in the HAE (Fig. 4A) and 60–80% of the cells in a given HAE culture are of the ciliated cell type [38], we estimate that only 10–20% of all ciliated cells in each culture were infected during inoculation. Infection of HAE with rHPIV2-WT produced maximum titers days 1–3 pi, which was demonstrated both by high levels of virus detected in the apical compartment and by the proportion of cells positive for HPIV2 antigen at those time points. The numbers of infected cells declined after day 3 and reached 50% of its peak by day 6 pi (Fig. 1C). The decline in the number of infected cells correlated with a reduction in viral titer determined at day 6 pi. Still, significant numbers of cells stained

positive for HPIV2 through day 6 pi, and viral shedding was detectable in the apical compartment through the final day of sampling.

Although apical inoculation of HAE by rHPIV2-WT did not result in basolateral shedding of virus, infection of HAE via the basolateral compartment was possible and resulted in increasing apical HPIV2 titers, indicating that this route of infection was productive (Fig. 2A). Following basolateral inoculation of HAE with rHPIV2-WT at a MOI of 5.0 TCID₅₀/cell, virus could be detected in the apical compartment at titers ranging from 10^{3.2} to 10^{5.2} TCID₅₀/ml by day 2 pi. To confirm that HPIV2 was indeed

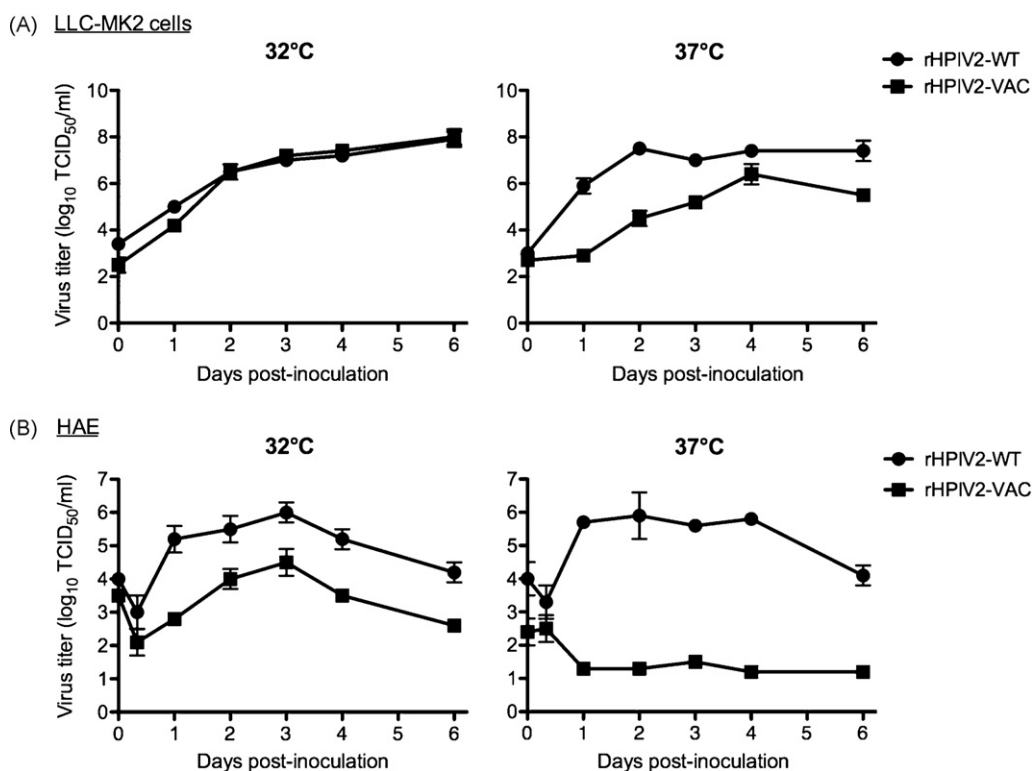


Fig. 3. Infection of LLC-MK2 cells and HAE with rHPIV2-WT and rHPIV2-VAC at temperatures reflective of the upper and lower airways. (A) Comparison of replication of rHPIV2-WT (circles) and rHPIV2-VAC (squares) in LLC-MK2 cells at 32 and 37 °C. Triplicate cell monolayers were infected at a MOI of 5.0 TCID₅₀/cell and aliquots were taken at 24-h intervals pi. The mean titer (log₁₀) for each time point is indicated. (B) Comparison of single cycle growth curves in HAE inoculated with rHPIV2-WT (circles) or rHPIV2-VAC (squares). HAE cells were inoculated at the apical surface with rHPIV2-WT or rHPIV2-VAC at a MOI of 5.0 TCID₅₀/cell. Cultures were incubated at either 32 or 37 °C, as indicated. Virus titers were determined in the apical compartments at the indicated times pi. Virus titers shown are the means of 6 cultures from 2 donors (3 cultures per donor) ± S.E., and the limit of detection is 1.2 log₁₀ TCID₅₀/ml.

able to infect HAE following basolateral exposure, we repeated this experiment at a lower MOI of rHPIV2-WT (1.0 TCID₅₀/cell). Again, rHPIV2-WT was observed to infect the HAE both apically and basolaterally as evidenced by detection of increasing virus titers in the apical wash samples (Fig. 2A). However, as virus titers in the basolateral compartment did not increase over the course of infection, HPIV2 appears to be shed primarily from the apical surface regardless of inoculation route (Fig. 2A). Additional cultures were inoculated (either apically or basolaterally) in parallel with rHPIV1-WT for comparison with rHPIV2-WT. Upon apical inoculation with rHPIV1-WT, robust HPIV1 shedding from the apical surface was detected, indicating productive infection of the HAE (Fig. 2A). As was previously reported [20], virus shedding into the basolateral compartment was not observed. Following basolateral inoculation with rHPIV1-WT, virus was detected at early time points (days 0–4 pi) in the basolateral wash samples, but the declining titer of virus during this period suggests that the virus detected represents residual inoculum and is not evidence of replication within the HAE. In contrast to our results for rHPIV2-WT, rHPIV1-WT virus shedding was not detected in the apical compartment of basolaterally infected HAE. Therefore, rHPIV1-WT infects the HAE after apical but not basolateral inoculation. The observation that rHPIV2-WT infected all cultures derived from four different donors via the basolateral surface, in contrast to HPIV1, which was not able to infect any of the cultures after basolateral inoculation, indicated that HPIV2 was capable of entering the HAE via apical and basolateral surfaces. *En face* immunostaining for HPIV2 and HPIV1 antigens verified that cells of the HAE were infected via both apical and basolateral inoculation with HPIV2 but not via basolateral inoculation with HPIV1 (Fig. 2B).

3.2. HAE reveal greater attenuation of rHPIV2-VAC growth than LLC-MK2 cells

The level of replication of rHPIV2-VAC and rHPIV2-WT was compared at 32 and 37 °C in LLC-MK2 cells and HAE to determine if HAE are able to detect the attenuation phenotype of rHPIV2-VAC that is not detected in LLC-MK2 cells. At 32 °C, the growth of rHPIV2-VAC in LLC-MK2 cells resembles that of rHPIV2-WT (Fig. 3A), whereas in HAE it is 30-fold lower than that of rHPIV2-WT (Fig. 3B). This indicates that HAE can detect a non-*ts att* phenotype that is not apparent in LLC-MK2 cells.

At 37 °C, the restriction of rHPIV2-VAC replication (compared with rHPIV2-WT) was much more pronounced in HAE (>10,000-fold) than in LLC-MK2 cells (10–100-fold) (Fig. 3A and B). The moderate restriction of replication of rHPIV2-VAC in LLC-MK2 cells at 37 °C is compatible with the presence of *ts att* mutations in the vaccine virus [29]. Clearly, the greater restriction of replication of rHPIV2-VAC in HAE at 37 °C indicates that HAE are the more sensitive of the two systems for the detection of the attenuating mutations in rHPIV2-VAC.

With regard to virus shedding from the basolateral surface following apical inoculation, rHPIV2-VAC behaved like rHPIV2-WT, i.e., it was not shed at either temperature (data not shown).

3.3. Type I interferon induction during HPIV2 infection of HAE

Epithelial cells lining the airways secrete cytokines and chemokines, which contribute to inflammatory pathology as well as to protective immune responses. It was previously demonstrated that infection of HAE with rHPIV1-WT did not induce significant levels of type I interferon (IFN) secretion, while infection with a

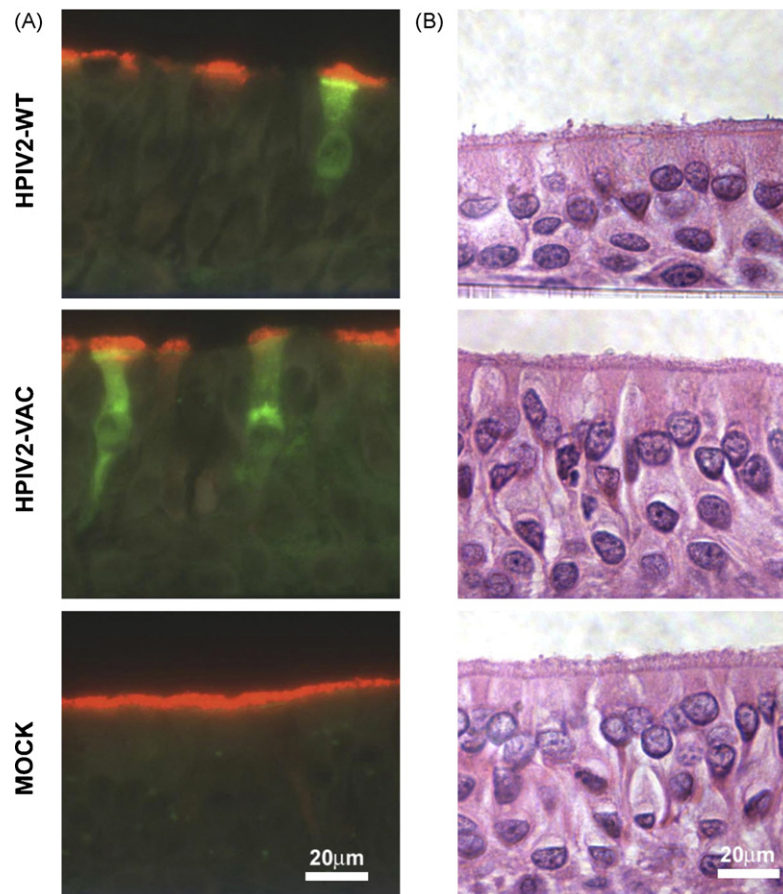


Fig. 4. HPIV2 infects ciliated cells in HAE cultures without causing obvious cytopathic effects or cell–cell fusion. (A) Photomicrographs of histological sections of HAE inoculated at a MOI of 5.0 TCID₅₀/cell with rHPIV2-WT (at 37 °C) or rHPIV2-VAC (at 32 °C) or with control fluid (mock). At day 6 pi, cells were fixed and prepared as histological sections and then immunoprobed with antibodies to HPIV2 (green) and acetylated alpha tubulin (red) to detect virus antigen and ciliated cells, respectively. HPIV2 antigen was detected only in ciliated columnar epithelial cells and not in mock-inoculated HAE. (B) Representative histological cross-sections of infected HAE counterstained with hematoxylin and eosin.

HPIV1 mutant encoding a defective HPIV1 IFN antagonist C protein induced high levels of IFN [20]. In these previous studies the induction of IFN correlated with the restriction of replication of the HPIV1 mutant in the HAE model. In the present study, we compared the concentration of type I IFN in the apical compartment following infection with rHPIV2-WT or rHPIV2-VAC to determine whether IFN played a role in the restriction of replication of either virus. Type I IFN was not (rHPIV2-VAC) or barely (rHPIV2-WT, 35 pg/ml IFN detected on day 4 only at 37 °C, lower limit of detection = 30 pg/ml) detectable in the apical compartment of cultures maintained at either 32 or 37 °C during the 6 days of study. This observation implies that a strong inhibition of IFN induction is operative in both WT and mutant HPIV2, supporting data from cell lines infected by HPIV2 [39–48]. These findings indicate that the attenuation of rHPIV2-VAC for HAE is mediated by mutations that do not directly involve IFN production and that the restricted replication of rHPIV2-VAC specified by the attenuated mutations might contribute to the weak IFN response.

3.4. HPIV2 infects ciliated cells in HAE without causing gross morphological changes

To determine the cell types targeted by HPIV2 and to characterize the effects of infection on airway epithelial cell morphology, histological cross-sections of HAE were stained for HPIV2 and acetylated alpha-tubulin, a marker of ciliated cells. Viral antigen was detected throughout the cytoplasm of cells that also stained

positive for acetylated alpha-tubulin, indicating that ciliated cells are infected by rHPIV2-WT, although not every ciliated cell was infected even at late time points (Fig. 4A). Ciliated cells were also infected following basolateral inoculation with HPIV2-WT (data not shown). Similar to rHPIV2-WT, rHPIV2-VAC also targeted ciliated cells of the HAE (Fig. 4A). Morphological assessment of histological cross-sections revealed that infection with HPIV2 did not induce gross changes in morphology or in the integrity of the epithelium when compared to the mock-inoculated cultures (Fig. 4B). Sections of HAE fixed on the final day of sampling (day 6) showed that neither rHPIV2-WT nor rHPIV2-VAC infection was associated with overt cytotoxicity or syncytia formation. In addition, mucociliary function determined by visual inspection of ciliary motion in infected HAE using a light microscope at each time point did not appear to be significantly compromised by HPIV2 infection. Alcian blue-PAS staining revealed slightly increased mucin production at 72 h pi in virus-infected cultures compared with mock-inoculated cultures (data not shown).

3.5. Cellular cytotoxicity induced by HPIV2 infection

We next evaluated whether infection with HPIV2 induced cytotoxicity in HAE that was undetectable by gross morphological analysis. Cytotoxicity can be evaluated by the quantification of plasma membrane damage resulting in the release of cytoplasmic contents into the extracellular space, i.e., the surrounding fluid. A ubiquitous cellular protein rapidly released into culture medium

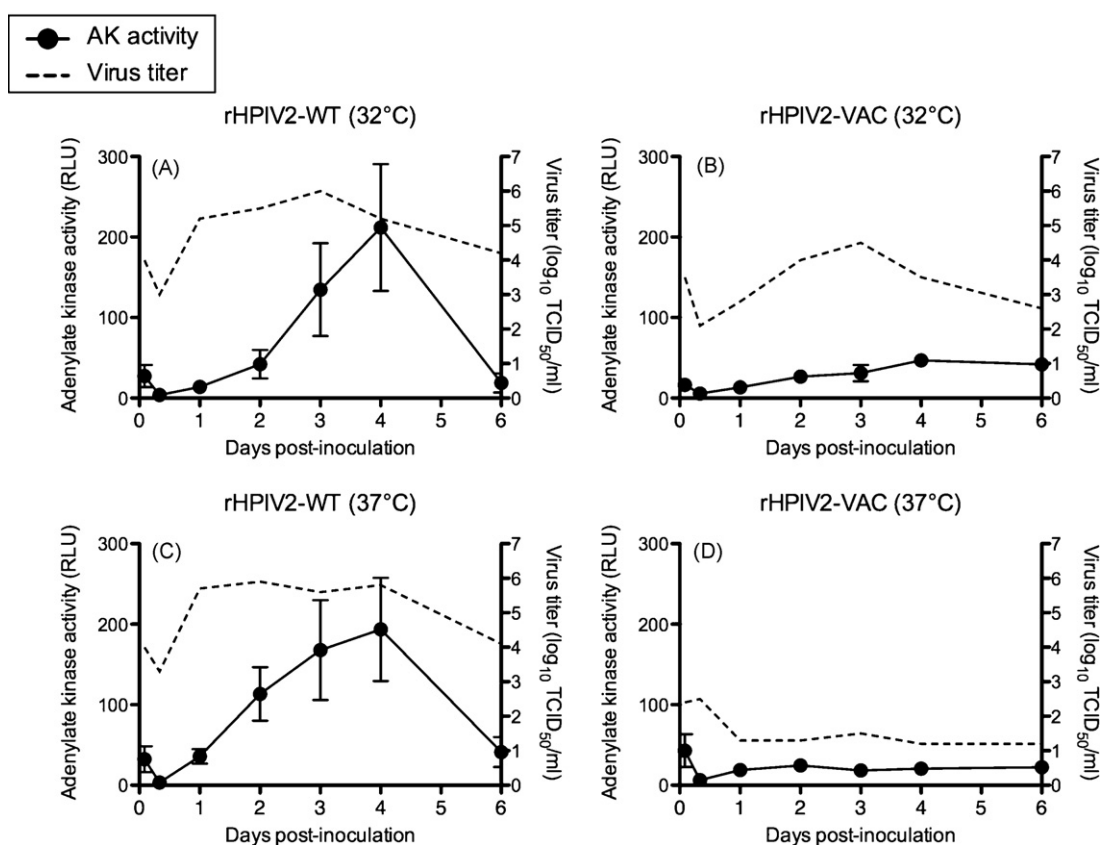


Fig. 5. Cellular cytotoxicity induced by HPIV2 infection. Cytotoxicity was quantified by measuring adenylate kinase activity in apical wash samples (circles, scale on left y-axis). Adenylate kinase in the sample activated a bioluminescent detection reagent (ToxiLight BioAssay Kit), which was detected using a luminometer; activity is expressed as relative luminescence units (RLU). Virus titers in the apical samples are shown as dashed lines for reference and use the same scale as Fig. 2A (scale on right y-axis).

as a result of plasma membrane damage is adenylate kinase (AK). By measuring AK activity in the same apical wash samples used to determine virus titers, it was possible to correlate the amount of progeny virus released with the level of cytotoxicity for that particular culture. For rHPIV2-WT infected HAE cultures maintained at either 32 or 37 °C (Fig. 5A and C, respectively), AK release peaked at day 4 pi, following peak levels of ongoing viral replication and correlating with lower virus titers at the same time point. However, infection with rHPIV2-VAC at either temperature induced minimal AK release (Fig. 5B and D), substantially less than that associated with rHPIV2-WT infection, indicating at the very least that increased virus replication correlated with increased AK release. No significant AK release was detected in mock-infected cultures that were handled identically (data not shown). The relatively transient increase in AK release in the rHPIV2-WT-infected HAE was not associated with significant alterations in the morphology of the epithelium in any of the cultures (Figs. 4 and 5, and data not shown).

3.6. Comparison of virus replication of rHPIV2-WT and rHPIV2-VAC vaccine candidate in African green monkeys and HAE

In order to determine whether attenuation in the HAE model correlated with the *att* phenotype of rHPIV2-VAC in AGMs, we compared rHPIV2-VAC and rHPIV2-WT virus titers in the apical washes of HAE and in the respiratory secretions of AGMs. For either virus, the mean virus titer in day 3 apical washes of HAE incubated at 32 °C was approximately 100-fold higher than the mean peak titer in the URT (upper respiratory tract, nasopharyngeal swab) of AGMs (Fig. 6A), and the difference was approximately 5-fold between HAE at 37 °C and the LRT (lower respiratory tract, tra-

cheal lavage fluid) of AGMs (Fig. 6B). The restriction of replication of rHPIV2-VAC versus rHPIV2-WT was 1.5 log₁₀ in the URT of AGMs ($P < 0.001$) and 1.6 log₁₀ in HAE cultures at 32 °C ($P < 0.01$) whereas it was 3.9 log₁₀ in the LRT of AGMs ($P < 0.001$) and 4.1 log₁₀ in HAE at 37 °C ($P < 0.001$), indicating a good correlation between the two systems for either temperature.

4. Discussion

The focus of this study was to characterize rHPIV2-WT infection in an in vitro model of HAE and to assess the utility of this model for evaluating phenotypes of candidate live attenuated virus vaccines. Although animal models have given important clues to the level of attenuation of potential vaccine strains, we sought to establish a human tissue culture system that reflects attenuation of respiratory virus vaccine candidates in seronegative humans. Towards this goal, we compared replication of a HPIV2 vaccine candidate currently in clinical trials and a WT HPIV2 virus in HAE and evaluated several factors that affect viral pathogenesis in the respiratory epithelium, including cytotoxicity, target cell type, polarity of virus release, and ability of these viruses to induce an IFN response.

The concept that HAE may be useful as a tool to correlate in vitro attenuation with in vivo attenuation is supported by studies in which attenuating mutations in several other respiratory viruses, including influenza A and B viruses, RSV, HPIV1 and HPIV3, all exhibited reduced growth in HAE compared to their parent strain [20,49–51]. Furthermore, data from these studies demonstrated a correlation between attenuation in HAE and attenuation in animal models and/or in seronegative children [50]. Specifically, levels of attenuation of two HPIV1 vaccine candidates exhibiting different levels of attenuation in AGMs was accurately reflected in HAE,

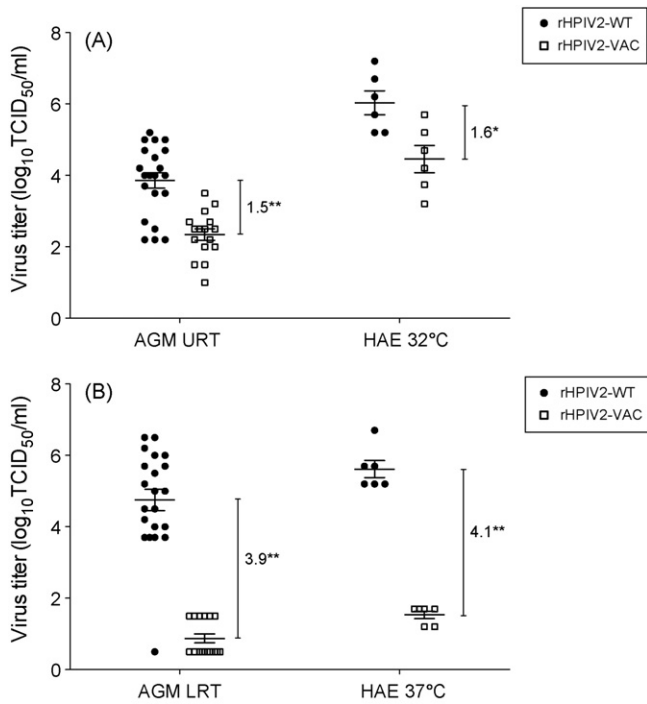


Fig. 6. Comparison of replication of rHPIV2-WT and rHPIV2-VAC in African green monkeys and HAE cultures. (A) Titers of rHPIV2-WT and rHPIV2-VAC in the URT (upper respiratory tract) of AGMs and in the apical wash of HAE incubated at 32 °C. (B) Virus titers in the LRT (lower respiratory tract) of AGMs and in the apical wash of HAE incubated at 37 °C. In both graphs, the peak virus titer, irrespective of sampling day, for each AGM is indicated by a circle (rHPIV2-WT infected AGMs) or square (rHPIV2-VAC infected AGMs). Virus titers from HAE were determined in high MOI growth curves (Fig. 3), and titers shown are from apical wash samples collected at day 3 pi. Lines indicate the mean peak titer for each group \pm S.E. A single asterisk (*) indicates statistical significance with P value > 0.01 , while (**) indicates a P value > 0.001 (two-way ANOVA with Bonferroni post-tests).

indicating the potential for evaluating respiratory virus vaccine candidates in this model [20,51]. Studies evaluating attenuation of investigational RSV vaccines also found a good correlation between their growth in HAE with that in chimpanzees and seronegative children [50].

In the current study, in a comparison with rHPIV2-WT, rHPIV2-VAC was restricted in replication in HAE to a level that closely mirrors its attenuation in vivo in AGMs. Mean peak titers of rHPIV2-VAC were 30–40-fold below rHPIV2-WT in both the URT of AGMs and in HAE at 32 °C. The restriction of rHPIV2-VAC replication in HAE at 32 °C was not observed in the non-polarized LLC-MK2 cell line, where its replication was equivalent to that of rHPIV2-WT at permissive temperature. Thus, rHPIV2-VAC contains a host range attenuating mutation that specifies attenuation (i.e., restricted replication) in AGMs and HAE (32 °C) but not in LLC-MK2 cells. We suggest that the restriction in replication of rHPIV2-VAC at the permissive temperature of 32 °C in HAE is due to the 15^{T-C} mutation in the 3' genomic promoter, which was shown previously to be a non-*ts* mutation that specifies attenuation in both the URT and LRT of AGMs [29]. In both HAE at 37 °C and the LRT of AGMs, rHPIV2-VAC replication was highly attenuated (approximately 10,000-fold lower titers than rHPIV2-WT) likely due to the additive effects of the non-*ts* and *ts* attenuating mutations [29]. The correlation between the extent of vaccine attenuation in HAE and AGMs further strengthens the concept that HAE models are useful for determining the attenuation phenotypes of potential respiratory virus vaccine candidates. Other recent data with a V-deletion mutant of HPIV2, rHPIV2-V^{ko}, also showed that attenuation of HPIV2 in vivo may be reflected in HAE, as this mutant was unable to grow

to detectable levels in either HAE or AGMs [52]. However, clear demonstration of a quantitative correlation between attenuation in vivo and in HAE will require more extensive testing of a panel of viruses with varying levels of attenuation in both systems. Once the safety, level of replication, and immunogenicity of rHPIV2-VAC is determined in seronegative children, the level of sensitivity of both the AGM and HAE models in identifying a satisfactory level of attenuation of rHPIV2-VAC for humans will be known. If the rHPIV2-VAC is under-attenuated for seronegative infants, viruses that are more attenuated than rHPIV2-VAC in comparative studies in HAE and/or AGMs will be selected for further evaluation in humans.

Our finding that the ciliated cells of HAE are permissive for HPIV2 infection is consistent with several other respiratory viruses including influenza A virus, SARS-CoV, RSV, HPIV1 and HPIV3 [20–23,53]. Although HPIV2 infection of HAE was less robust than that of HPIV1 and HPIV3 [20,21], HAE clearly supported HPIV2 replication with amplification of virus titer and can therefore be used to model characteristics of HPIV2 infection of the human respiratory tract in vivo. The level of HPIV2 replication in HAE correlates with that seen in human cell lines [52], and may be a reflection of the lower incidence of severe disease associated with the virus versus the other HPIVs [2].

The ability of rHPIV2-VAC to infect HAE at 32 °C and to replicate to a peak titer of approximately 10^{4.5} TCID₅₀/ml suggests that this virus will productively infect the upper respiratory tract of humans, thereby triggering an adaptive immune response in the vaccine. In addition to its restricted replication, we observed a decline in virus titers from day 3 onward, indicating that, even in the absence of immune cells and a humoral immune response, virus replication is restricted by the innate epithelial immune system. Initially, we suspected that this decrease in virus shedding might be due to the production of cytokines and other immune mediators by the epithelial cells that suppress virus growth. Previous studies with HPIV1 mutants possessing mutations that disable the viral IFN antagonist genes indicated that type I IFN secreted by HAE cells was capable of reducing replication of viruses that were rendered susceptible to the antiviral effects of IFN [20]. However, our evaluation of the type I IFN response showed no link between IFN production in HAE and the reduction of HPIV2 replication, though this does not rule out a contribution of other innate epithelial cell responses to limiting virus replication. This was not surprising since rHPIV2-VAC does not possess mutations in the V protein, the known IFN antagonist gene of HPIV2. Rather, the failure to detect IFN in the cultures of rHPIV2-VAC infected cells reflects the restricted replication of this virus imposed by the mutations in L and the 3' genomic promoter. Future studies in HAE will likely further our understanding of both the innate immune responses of airway epithelial cells that limit the extent and duration of respiratory virus infection and the mechanisms by which host range mutations, such as the 15^{T-C} mutation, restrict replication in human ciliated epithelial cells.

In addition to cytokine production, in vivo infection with respiratory viruses can cause dramatic changes in the respiratory epithelium. For example, influenza virus infection results in dramatic cytopathic effects in the columnar cells of HAE cultures within 48 h, with early cessation of ciliary beat and eventual loss of columnar epithelial cells, although basal epithelial cells are spared [24,26]. In contrast, cytopathology induced in HAE by HPIV1, HPIV3, and RSV infections is much more subtle than that induced by influenza viruses [21,22]. Similarly, infection of HAE with HPIV2 did not induce syncytia formation or disruption of overall mucociliary function, and epithelial integrity was not dramatically altered compared to uninfected cultures from the same donor. However, these observations may be due partly to the low number of cells infected in each culture as cytotoxicity assays detected some alterations in the HAE that were not observed in histological analyses. This cytotoxicity could be due either to the death of infected cells

by cytopathic effect of viral infection or by cellular apoptotic mechanisms. In contrast to rHPIV2-WT, rHPIV2-VAC exhibited minimal cytotoxicity determined by AK release, corresponding to lower levels of replication.

In the polarized HAE model, the apical compartment represents the airway lumen, while the basolateral compartment represents the interstitial and vascular support of the lungs. Because HPIV vaccines are being developed for intranasal inoculation, vaccine strains must be able to productively infect apical, or luminal, cell surfaces for intranasal administration. Our studies confirmed that inoculation of the apical surface of HAE is a productive route of infection for rHPIV2-VAC, which supports intranasal inoculation as a means of vaccination. Interestingly, HPIV2 also appears to be able to enter the HAE via the basolateral surface. Other paramyxoviruses, such as measles virus (genus *Morbillivirus*), can also enter HAE via the basolateral surface yet, like HPIV2, measles virus is released primarily apically [25,54,55]. Whether the ability of HPIV2 to infect HAE after basolateral inoculation is of biological significance is unknown as no indication of HPIV2 viremia has been reported and signs of systemic illness (other than fever) are not seen in immunocompetent individuals [56].

Significantly, following inoculation with rHPIV2-WT or rHPIV2-VAC, virus shedding appears to be primarily at the apical side of the polarized HAE cultures. In vivo, this would result in shedding into the lumen and away from underlying tissues, increasing the likelihood that infection will remain localized to epithelial surfaces in the respiratory tract. Although apical budding is not the only mechanism that restricts systemic spread of a virus, a similar restriction of virus release to apical surfaces has also been seen previously with the related parainfluenza viruses HPIV1 and HPIV3, as well as RSV and influenza A virus, and is consistent with the pattern of infection limited to the respiratory tract that is typically seen throughout the course of disease during human infection with HPIV2 [20–22,24]. Clinical data also indicate that WT HPIV2 is shed lumenally and present in respiratory secretions whereas viremia or replication at distant sites has not been reported [57]. Similarly, HPIV2 viremia was not detectable in spite of high titer replication in the URT and LRT of AGM (unpublished data, ASN, ACS, and BRM). The observation that rHPIV2-VAC is released from the apical surface is important for vaccine development because it will unlikely cause viremia or spread to systemic organs in vaccines.

In summary, the rHPIV2-VAC investigational vaccine has been characterized extensively in HAE and in AGMs and was highly attenuated in both. This study extended analysis of rHPIV2-VAC to a human in vitro model system that is likely predictive of HPIV replication in the airways of seronegative children and demonstrated a consistent, high level of attenuation for rHPIV2-VAC in human ciliated epithelial cells at 37 °C, indicating that it is very unlikely to cause severe lower respiratory disease in seronegative children. The close correlation between limited growth of rHPIV2-VAC versus that of rHPIV2-WT in both AGMs and in HAE provides additional evidence that this virus will be attenuated in humans. Since rHPIV2-VAC is currently being evaluated in clinical trials as a live attenuated vaccine candidate for HPIV2, it will be valuable to compare data generated in HAE models to levels of replication in seronegative humans in order to fully assess the correlation between the level of attenuation of a vaccine candidate in the HAE model versus that in humans. If the clinical trials indicate that additional HPIV2 vaccine candidates need to be developed, HAE and rHPIV2-VAC can be used together to assess which candidates have favorable attenuation profiles for clinical development.

Acknowledgements

We thank the directors and teams of the UNC Cystic Fibrosis Center Tissue Culture Core, the Morphology and Morphometry Core,

and the Michael Hooker Microscopy Facility for supplying reagents and technical expertise. We also thank Susan Burkett and Emerito Amaro-Carambot for technical assistance. This research was supported by the Intramural Research Program of the NIH, NIAID, and by NIH grant R01 HL77844 (RJP) and the Molecular Biology of Viral Diseases Training Grant 5-T32-AI007419.

References

- [1] Karron RA, Collins PL. Parainfluenza viruses. In: Knipe DM, Howley PM, editors. *Fields virology*. 5th ed. Philadelphia: Lippincott Williams & Wilkins; 2007. p. 1497–526 (chapter 42).
- [2] Murphy BR. Current approaches to the development of vaccines effective against parainfluenza viruses. *Bull World Health Organ* 1988;66(3):391–7.
- [3] Weinberg GA, Hall CB, Iwane MK, Poehling KA, Edwards KM, Griffin MR, et al. Parainfluenza virus infection of young children: estimates of the population-based burden of hospitalization. *J Pediatr* 2009;154(May (5)):694–9.
- [4] Forster J, Ithorst G, Rieger CH, Stephan V, Frank HD, Gurth H, et al. Prospective population-based study of viral lower respiratory tract infections in children under 3 years of age (the PRI.DE study). *Eur J Pediatr* 2004;163(December (12)):709–16.
- [5] Murphy BR. Mucosal immunity to viruses. In: Ogra PL, Mestecky J, Lamm ME, Strober W, McGhee JR, Bienstock J, editors. *Mucosal immunology*. 2nd ed. Academic Press, Inc.; 1999. p. 695–707.
- [6] Karron RA, Belshe RB, Wright PF, Thumar B, Burns B, Newman F, et al. A live human parainfluenza type 3 virus vaccine is attenuated and immunogenic in young infants. *Pediatr Infect Dis J* 2003;22(May (5)):394–405.
- [7] Compans RW, Herrler G. Virus infection of epithelial cells. In: Mestecky J, Lamm ME, Strober W, Bienstock J, McGhee JR, Mayer L, editors. *Mucosal immunology*. 3rd ed. Amsterdam, Boston: Elsevier Academic Press; 2005. p. 769–80 (chapter 41).
- [8] Tremonti LP, Lin JS, Jackson GG. Neutralizing activity in nasal secretions and serum in resistance of volunteers to parainfluenza virus type 2. *J Immunol* 1968;101(3):572–7.
- [9] Mossad SB. Demystifying FluMist, a new intranasal, live influenza vaccine. *Cleve Clin J Med* 2003;70(September (9)):801–6.
- [10] Karron RA, Wright PF, Belshe RB, Thumar B, Casey R, Newman F, et al. Identification of a recombinant live attenuated respiratory syncytial virus vaccine candidate that is highly attenuated in infants. *J Infect Dis* 2005;191(April (7)):1093–104.
- [11] Belshe RB, Newman FK, Tsai TF, Karron RA, Reisinger K, Robertson D, et al. Phase 2 evaluation of parainfluenza type 3 cold passage mutant 45 live attenuated vaccine in healthy children 6–18 months old. *J Infect Dis* 2004;189(February (3)):462–70.
- [12] Karron RA, Wright PF, Newman FK, Makhene M, Thompson J, Samorodin R, et al. A live human parainfluenza type 3 virus vaccine is attenuated and immunogenic in healthy infants and children. *J Infect Dis* 1995;172(6):1445–50.
- [13] Bracco Neto H, Farhat CK, Tregnaighi MW, Madhi SA, Razmpour A, Palladino G, et al. Efficacy and safety of 1 and 2 doses of live attenuated influenza vaccine in vaccine-naïve children. *Pediatr Infect Dis J* 2009;28(May (5)):365–71.
- [14] Johnson JE, Gonzales RA, Olson SJ, Wright PF, Graham BS. The histopathology of fatal untreated human respiratory syncytial virus infection. *Mod Pathol* 2007;20(January (1)):108–19.
- [15] Madden JF, Burchette Jr JL, Hale LP. Pathology of parainfluenza virus infection in patients with congenital immunodeficiency syndromes. *Hum Pathol* 2004;35(May (5)):594–603.
- [16] Parrott R, Vargosko A, Kim HW, Bell J, Chanock R. Myxoviruses III parainfluenza. *Am J Public Health* 1962;52:907–17.
- [17] Parrott R, Vargosko A, Luckey A, Kim H, Cumming C, Chanock R. Clinical features of infection with hemadsorption viruses. *N Engl J Med* 1959;260:731–8.
- [18] Matsui H, Grubb BR, Tarran R, Randell SH, Gatzky JT, Davis CW, et al. Evidence for periciliary liquid layer depletion, not abnormal ion composition, in the pathogenesis of cystic fibrosis airways disease. *Cell* 1998;95(December (7)):1005–15.
- [19] Pickles RJ, McCarty D, Matsui H, Hart PJ, Randell SH, Boucher RC. Limited entry of adenovirus vectors into well-differentiated airway epithelium is responsible for inefficient gene transfer. *J Virol* 1998;72(July (7)):6014–23.
- [20] Bartlett EJ, Hennessey M, Skiadopoulos MH, Schmidt AC, Collins PL, Murphy BR, et al. The role of interferon in the replication of human parainfluenza virus type 1 wild type and mutant viruses in human ciliated airway epithelium. *J Virol* 2008;82(June (16)):8059–70.
- [21] Zhang L, Bukreyev A, Thompson CI, Watson B, Peebles ME, Collins PL, et al. Infection of ciliated cells by human parainfluenza virus type 3 in an in vitro model of human airway epithelium. *J Virol* 2005;79(January (2)):1113–24.
- [22] Zhang L, Peebles ME, Boucher RC, Collins PL, Pickles RJ. Respiratory syncytial virus infection of human airway epithelial cells is polarized, specific to ciliated cells, and without obvious cytopathology. *J Virol* 2002;76(June (11)):5654–66.
- [23] Sims AC, Baric RS, Yount B, Burkett SE, Collins PL, Pickles RJ. Severe acute respiratory syndrome coronavirus infection of human ciliated airway epithelia: role of ciliated cells in viral spread in the conducting airways of the lungs. *J Virol* 2005;79(December (24)):15511–24.
- [24] Thompson CI, Barclay WS, Zambon MC, Pickles RJ. Infection of human airway epithelium by human and avian strains of influenza A virus. *J Virol* 2006;80(August (16)):8060–8.

- [25] Leonard VH, Sinn PL, Hodge G, Miest T, Devaux P, Oezguen N, et al. Measles virus blind to its epithelial cell receptor remains virulent in rhesus monkeys but cannot cross the airway epithelium and is not shed. *J Clin Invest* 2008;118(July (7)):2448–58.
- [26] Taubenberger JK, Morens DM. The pathology of influenza virus infections. *Annu Rev Pathol* 2008;3:499–522.
- [27] Nolan SM, Surman SR, Amaro-Carambot E, Collins PL, Murphy BR, Skiadopoulos MH. Live-attenuated intranasal parainfluenza virus type 2 vaccine candidates developed by reverse genetics containing L polymerase protein mutations imported from heterologous paramyxoviruses. *Vaccine* 2005;39(September (23)):4765–74.
- [28] Skiadopoulos MH, Vogel L, Riggs JM, Surman SR, Collins PL, Murphy BR. The genome length of human parainfluenza virus type 2 follows the rule of six, and recombinant viruses recovered from non-polyhexameric-length antigenomic cDNAs contain a biased distribution of correcting mutations. *J Virol* 2003;77(January (1)):270–9.
- [29] Nolan SM, Skiadopoulos MH, Bradley K, Kim OS, Bier S, Amaro-Carambot E, et al. Recombinant human parainfluenza virus type 2 vaccine candidates containing a 3' genomic promoter mutation and L polymerase mutations are attenuated and protective in non-human primates. *Vaccine* 2007;25(August (34)):6409–22.
- [30] Skiadopoulos MH, Schmidt AC, Riggs JM, Surman SR, Elkins WR, St Claire M, et al. Determinants of the host range restriction of replication of bovine parainfluenza virus type 3 in rhesus monkeys are polygenic. *J Virol* 2003;77(January (2)):1141–8.
- [31] Bartlett EJ, Amaro-Carambot E, Surman SR, Newman JT, Collins PL, Murphy BR, et al. Human parainfluenza virus type 1 (HPIV1) vaccine candidates designed by reverse genetics are attenuated and efficacious in African green monkeys. *Vaccine* 2005;23(September (38)):4631–46.
- [32] Murphy BR, Richman DD, Chalhub EG, Uhlenendorf CP, Baron S, Chanock RM. Failure of attenuated temperature-sensitive influenza A (H3N2) virus to induce heterologous interference in humans to parainfluenza type 1 virus. *Infect Immun* 1975;12(1):62–8.
- [33] Chanock R, Parrott R, Johnson K, Kapikian A, Bell J. Myxoviruses: parainfluenza. *Am Rev Respir Dis* 1963;88:152–66.
- [34] Clemons DJ, Besch-Williford C, Steffen EK, Riley LK, Moore DH. Evaluation of a subcutaneously implanted chamber for antibody production in rabbits. *Lab Anim Sci* 1992;42(3):307–11.
- [35] Park MS, Garcia-Sastre A, Cros JF, Basler CF, Palese P. Newcastle disease virus V protein is a determinant of host range restriction. *J Virol* 2003;77(September (17)):9522–32.
- [36] Stojdl DF, Lichty BD, tenOver BR, Paterson JM, Power AT, Knowles S, et al. VSV strains with defects in their ability to shutdown innate immunity are potent systemic anti-cancer agents. *Cancer Cell* 2003;4(October (4)):263–75.
- [37] Scull MA, Gillim-Ross L, Santos C, Roberts KL, Bordonali E, Subbarao K, et al. Avian Influenza virus glycoproteins restrict virus replication and spread through human airway epithelium at temperatures of the proximal airways. *PLoS Pathog* 2009;5(May (5)):e1000424.
- [38] Zhang L, Button B, Gabriel SE, Burkett S, Yan Y, Skiadopoulos MH, et al. CFTR delivery to 25% of surface epithelial cells restores normal rates of mucus transport to human cystic fibrosis airway epithelium. *PLoS Biol* 2009;7(July (7)):e1000155.
- [39] Lu LL, Puri M, Horvath CM, Sen GC. Select paramyxoviral V proteins inhibit IRF3 activation by acting as alternative substrates for inhibitor of kappaB kinase epsilon (IKKe)/TBK1. *J Biol Chem* 2008;283(May (21)):14269–76.
- [40] Andrejeva J, Childs KS, Young DF, Carlos TS, Stock N, Goodbourn S, et al. The V proteins of paramyxoviruses bind the IFN-inducible RNA helicase, mda-5, and inhibit its activation of the IFN-beta promoter. *Proc Natl Acad Sci USA* 2004;101(December (49)):17264–9.
- [41] Andrejeva J, Young DF, Goodbourn S, Randall RE. Degradation of STAT1 and STAT2 by the V proteins of simian virus 5 and human parainfluenza virus type 2, respectively: consequences for virus replication in the presence of alpha/beta and gamma interferons. *J Virol* 2002;76(March (5)):2159–67.
- [42] Parisien JP, Lau JF, Rodriguez JJ, Sullivan BM, Moscona A, Parks GD, et al. The V protein of human parainfluenza virus 2 antagonizes type I interferon responses by destabilizing signal transducer and activator of transcription 2. *Virology* 2001;283(2):230–9.
- [43] Parisien JP, Lau JF, Horvath CM. STAT2 acts as a host range determinant for species-specific paramyxovirus interferon antagonism and simian virus 5 replication. *J Virol* 2002;76(July (13)):6435–41.
- [44] Parisien JP, Lau JF, Rodriguez JJ, Ulane CM, Horvath CM. Selective STAT protein degradation induced by paramyxoviruses requires both STAT1 and STAT2 but is independent of alpha/beta interferon signal transduction. *J Virol* 2002;76(May (9)):4190–8.
- [45] Precious B, Young DF, Andrejeva L, Goodbourn S, Randall RE. In vitro and in vivo specificity of ubiquitination and degradation of STAT1 and STAT2 by the V proteins of the paramyxoviruses simian virus 5 and human parainfluenza virus type 2. *J Gen Virol* 2005;86(January (Pt 1)):151–8.
- [46] Ulane CM, Kentsis A, Cruz CD, Parisien JP, Schneider KL, Horvath CM. Composition and assembly of STAT-targeting ubiquitin ligase complexes: paramyxovirus V protein carboxyl terminus is an oligomerization domain. *J Virol* 2005;79(August (16)):10180–9.
- [47] Nishio M, Garcin D, Simonet V, Kolakofsky D. The carboxyl segment of the mumps virus V protein associates with Stat proteins in vitro via a tryptophan-rich motif. *Virology* 2002;300(August (1)):92–9.
- [48] Nishio M, Tsurudome M, Ito M, Kawano M, Komada H, Ito Y. High resistance of human parainfluenza type 2 virus protein-expressing cells to the antiviral and anti-cell proliferative activities of alpha/beta interferons: cysteine-rich V-specific domain is required for high resistance to the interferons. *J Virol* 2001;75(19):9165–76.
- [49] Wright PF, Ikizler M, Carroll KN, Endo Y. Interactions of viruses with respiratory epithelial cells. *Semin Virol* 1996;7:227–35.
- [50] Wright PF, Ikizler MR, Gonzales RA, Carroll KN, Johnson JE, Werkhaven JA. Growth of respiratory syncytial virus in primary epithelial cells from the human respiratory tract. *J Virol* 2005;79(July (13)):8651–4.
- [51] Bartlett EJ, Cruz AM, Esker J, Castano A, Schomacker H, Surman SR, et al. Human parainfluenza virus type 1C proteins are nonessential proteins that inhibit the host interferon and apoptotic responses and are required for efficient replication in nonhuman primates. *J Virol* 2008;82(September (18)):8965–77.
- [52] Schaap-Nutt A, D'Angelo C, Scull M, Amaro-Carambot E, Nishio M, Pickles R, et al. Human parainfluenza virus type 2 V protein inhibits interferon production and signaling and is required for replication in non-human primates. *Virology* 2010;397:285–98.
- [53] Matrosovich MN, Matrosovich TY, Gray T, Roberts NA, Klenk HD. Human and avian influenza viruses target different cell types in cultures of human airway epithelium. *Proc Natl Acad Sci USA* 2004;101(March (13)):4620–4.
- [54] Blau DM, Compans RW. Entry and release of measles virus are polarized in epithelial cells. *Virology* 1995;210(June (1)):91–9.
- [55] Maisner A, Klenk H, Herrler G. Polarized budding of measles virus is not determined by viral surface glycoproteins. *J Virol* 1998;72(6):5276–8.
- [56] Kapikian A, Bell J, Mastrotta F, Huebner R, Wong D, Chanock R. An outbreak of parainfluenza 2 (croup-associated) virus infection. *JAMA* 1963;183:324–30.
- [57] Taylor-Robinson D, Bynoe ML. Para-influenza 2 virus infections in adult volunteers. *J Hyg (Lond)* 1963;61(December):407–17.